Medical Imaging
with
High Performance Computing

Efstathios Stiliaris
Department of Physics, University of Athens
&
Inst. of Accelerating Systems and Applications (IASA)

9th February 2009

Users Meeting in Athens, OTE Academy

LINKSCEEM

X-Ray Transmission Computed Tomography

CT Technology

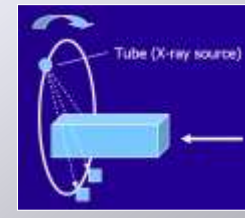

Classified by the Beam Geometry

- Parallel Beam
- Cone Beam
- Fan Beam

Classified by the X-Ray Locus

- Circle
- Spiral

Single Photon Emission Computed Tomography (SPECT)
&
Positron Emission Tomography (PET)

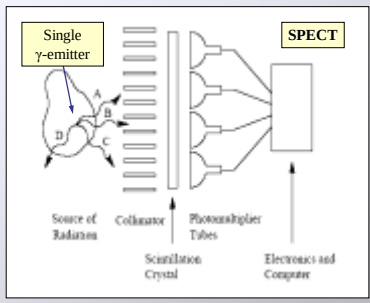

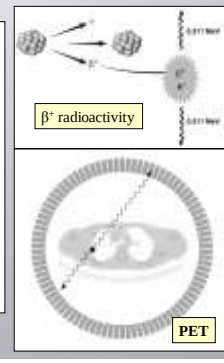

Multimodalities

CT Image (X-rays)

PET/CT fused images showing non-small cell lung carcinoma

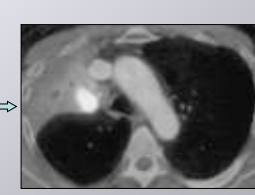

PET Image

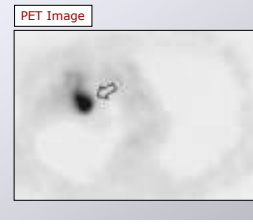

Antoch G. *et al.*, Radiology 229 (2003) 526

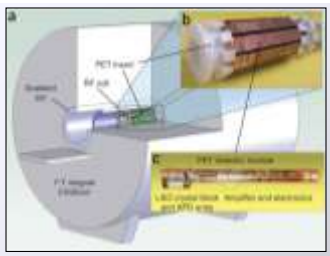

Multimodalities

Simultaneous PET-MRI

A new approach for functional and morphological imaging

Nature Medicine 14 (2008) 459-465

PET Image

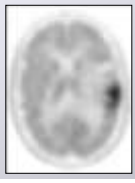

+

MRI Image

Fused Image

Small Animal Cameras

The small field, high-resolution γ-Camera system for SPECT at IASA.

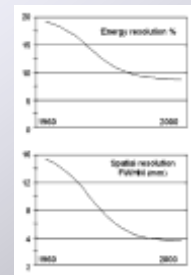

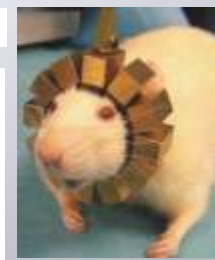

RatCAP

A small, head-mounted PET tomograph for imaging the brain of an awake RAT

C. Woody *et al.*
Brookhaven National Laboratory

N. Giokaris et al., Nucl. Instrum. & Methods A 497 (2003) 141

Small Animal Cameras

MEDIPIX2
Semiconductor single-particle-counting pixel detector for X- and γ-radiation imaging

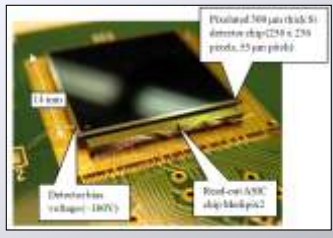

CERN Medipix2 Collaboration

Ground beetle X-ray transmission image

COMPUTED TOMOGRAPHY

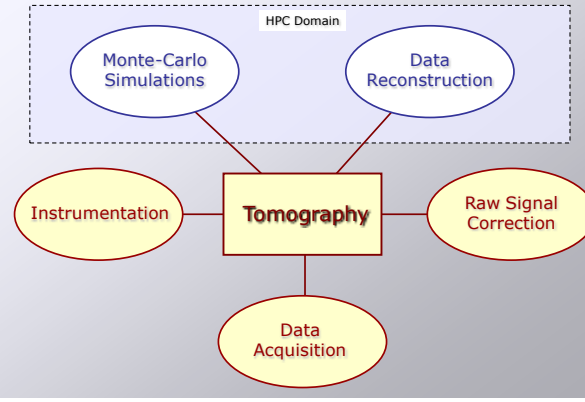

Tomographic Image Reconstruction

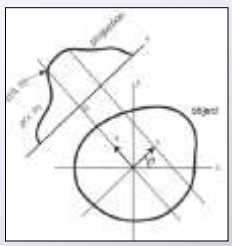

$$g(\theta,s)=\int_{-\infty}^{\infty} f(x\cos\theta-u\sin\theta, x\sin\theta+u\cos\theta)\,du$$

$$\begin{bmatrix} s \\ u \end{bmatrix} = \begin{bmatrix} \cos\theta & \sin\theta \\ -\sin\theta & \cos\theta \end{bmatrix} \begin{bmatrix} x \\ y \end{bmatrix} \quad \begin{bmatrix} x \\ y \end{bmatrix} = \begin{bmatrix} \cos\theta & -\sin\theta \\ \sin\theta & \cos\theta \end{bmatrix} \begin{bmatrix} s \\ u \end{bmatrix}$$

Radon Transform

$$f(x,y) = \int_0^{2\pi} g(\theta,s)\,d\theta$$

J. Radon (1917)
Über die Bestimmung von Funktionen durch ihre Integralwerte längs gewisser Mannigfaltigkeiten.

Berichte Sächsischer Akademie der Wissenschaften, Math. Phys. Klass. v69. 262-277

Tomographic Image Reconstruction

Tomographic Reconstruction from Planar Images

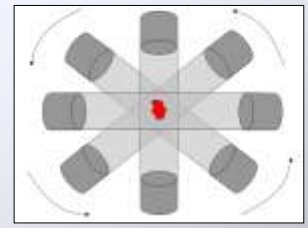

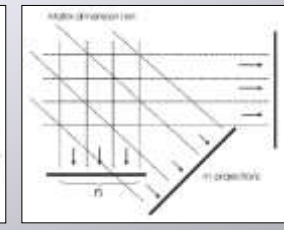

Problem Definition
Reconstruct the n×n matrix from the m×n projections

Tomographic Image Reconstruction

Reconstruction Algorithms

- Analytic Algorithms
  - Fourier Inversion, Filtered Back Projection
- Iterative Algorithms
  - Algebraic Reconstruction Technique (ART)
  - Maximum Likelihood – Expectation Maximization (MLEM)
- Artificial Neural Networks (ANN)

Tomographic Image Reconstruction

Parallel Implementation of the Filtered Back Projection Algorithm

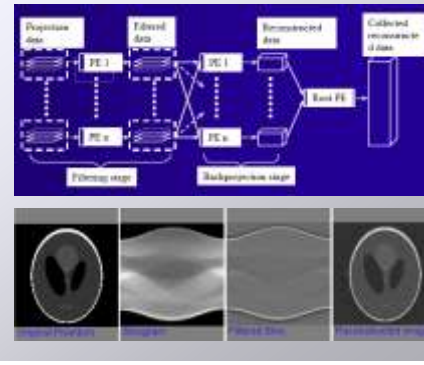

Tomographic Image Reconstruction

Reconstruction of a 3D Shepp-Logan Phantom

TIME

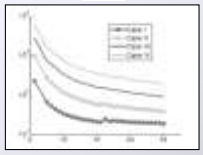

Case I : 128^3 Case III : 384^3
Case II : 256^3 Case IV : 512^3

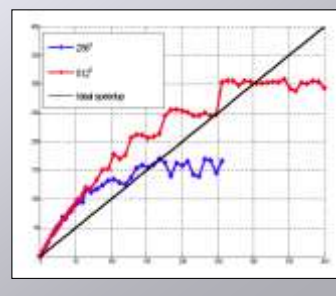

SPEED UP

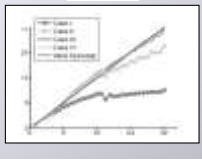

Tomographic Image Reconstruction

Iterative Algorithms

Reconstruction of the N × N Matrix from M Projections

Algebraic Reconstruction Technique (ART)

$$x_j^{new} = x_j^{old} + P_{i,j}\frac{R_i - R_i^{old}}{N_i}$$

M × N steps per Iteration

Maximum Likelihood – Expectation Maximization (MLEM)

$$x_j^{new} = x_j^{old}\left(\frac{\sum_i P_{i,j}\dfrac{R_i}{\sum_k P_{i,k}x_k}}{\sum_i P_{i,j}}\right)$$

N × N steps per Iteration

Tomographic Image Reconstruction

Iterative Algorithms

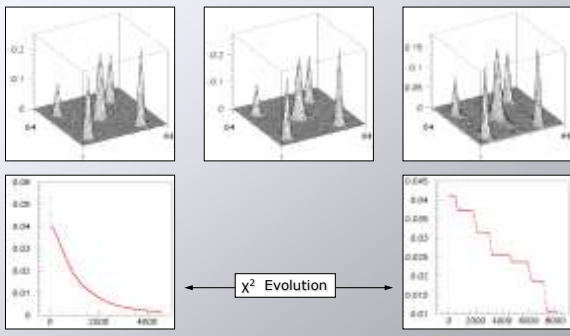

ART MLEM

Tomographic Image Reconstruction

Usage of Artificial Neural Network (ANN) Techniques

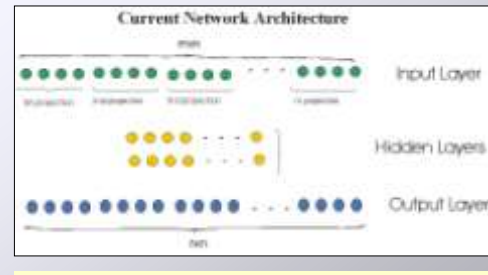

M × N

K

N × N

Total Number of Synapses

- No hidden layer (N × N) · (M × N) ~ N^3
- One hidden layer (M × N × k) + (k × N × N) ~ N^2

Tomographic Image Reconstruction

Training of the Neural Network

Picture Size	**64 ✥ 64**
Num of Projections	**18**
INPUT nodes	**18 ✥ 64**
OUTPUT nodes	**64 ✥ 64**
TOTAL synapses	**18 ✥ 64^3**
Training Time per cycle (P4-3GHz)	**30min**

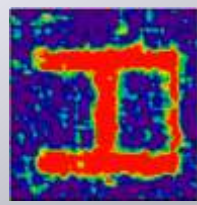

Cycle 378

Drawback: Large Training Time

Advantage: Direct Response in any Input Signal after Training

Tomographic Image Reconstruction

Simulation Results: Reconstruction of the Shepp Logan phantom

ORIGINAL NEURAL NET ART

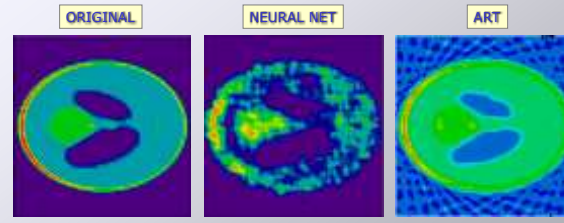

Reconstruction Time: 0.02 sec 54 sec

Ch. Tsoumpas, Diploma Thesis, UoA (2002)

Tomographic Image Reconstruction

ANN Test Results with Phantoms (Capillaries filled with ^{99m}Tc)

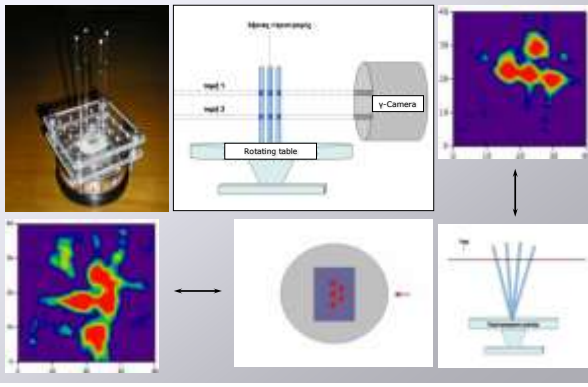

Monte Carlo: GEANT4/GATE Simulation Tools

Geant4 is a toolkit for the simulation of the passage of particles through matter. Its areas of application include high energy, nuclear and accelerator physics, as well as studies in medical and space science.

GATE (Geant4 Application for Emission Tomography) incorporates the Geant4 libraries in a modular, versatile, and scripted simulation toolkit which is adapted to the field of nuclear medicine. In addition, GATE allows the accurate description of time-dependent phenomena such as source or detector movement and source decay kinetics.

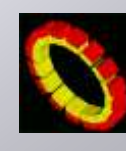

Monte Carlo: GEANT4/GATE PET Simulation

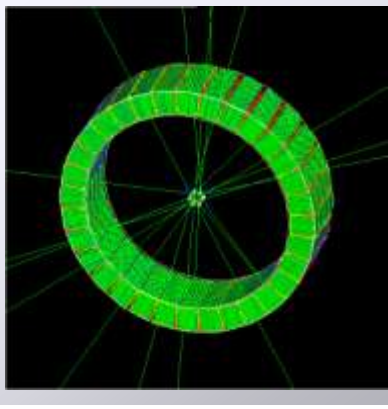

KI
Water Solution
1.10 – 1.05 – 1.025 g/cm³

$CaCl_2$
Water Solution
1.10 – 1.05 – 1.025 g/cm3

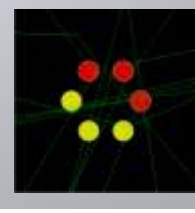

Monte Carlo: GEANT4/GATE PET Simulation

Position Reconstruction Results

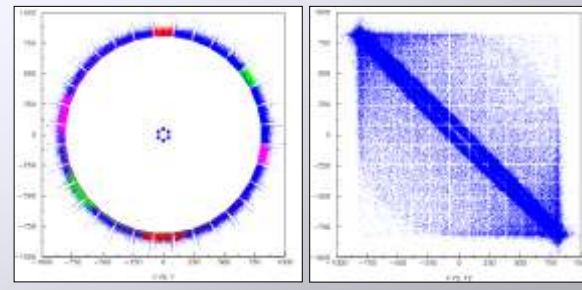

Detected $\gamma_1 - \gamma_2$ Photon Correlations

G. Hantzopoulos, Diploma Thesis, UoA (2008)

Monte Carlo: GEANT4/GATE PET Simulation

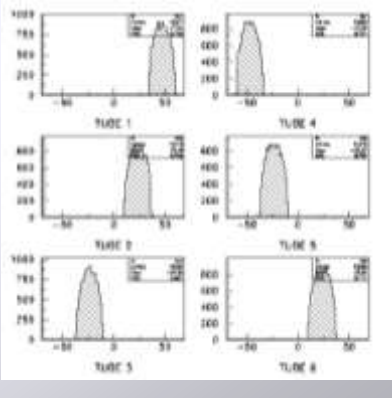

Simulation Results

Detected relative activities for each tube

KI Solution		
1	2	3
1.000	0.992	1.002
$CaCl_2$ Solution		
4	5	6
0.997	1.004	0.996

Monte Carlo: GEANT4/GATE SPECT Simulation

Focus effects of the collimator – Comparison with experimental results

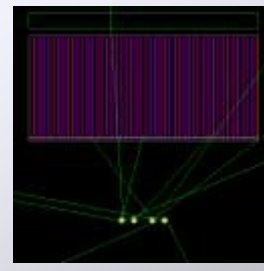

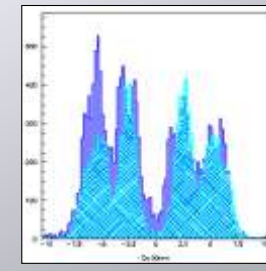

J. Kyriakidou and M. Mikeli, Diploma Theses, UoA (2007)

Monte Carlo: GEANT4/GATE SPECT Simulation

• Energy spectra obtained for a ^{99m}Tc point source under water.

• Comparison with experimental results taken with the IASA γ-Camera for different water depths.

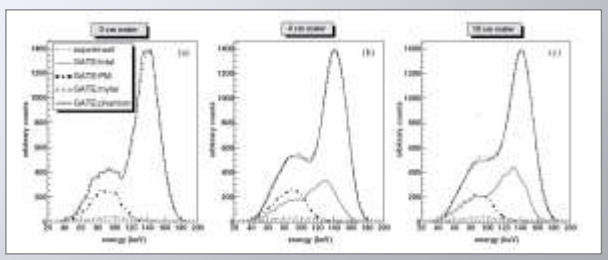

D. Lazaro *et al.*, Phys. Med. Biol. 49 (2003) 271

Monte Carlo: Optical Simulation

Pixelated Scintillation Crystal CsI(Tl)

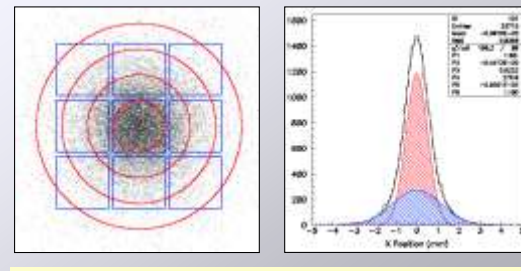

Study of the photon transport in the optical media with the software package **DETECT2000**

M. Mikeli *et al.*, IEEE NSS-MIC (2008) 4736-4741

Monte Carlo: Voxelized Phantoms

Attenuation Effects

$$I = I_0 e^{-\int u(x)dx}$$

Attenuation Coefficient u(x) depends on material composition.

Analytically defined thorax phantom and transverse image of its voxelized (256^3) counterpart.

Voxelized phantoms can accurately model detailed human shapes based on segmented CT or MRI images.

J. Peter, IEEE TMI 19 (2000) 8

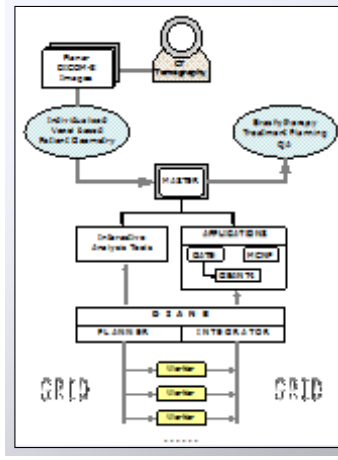

Monte-Carlo Calculations for Brachytherapy Treatment

Brachytherapy treatment planning based on accurate dosimetric studies taking in account:

• Individualized Voxel based Patient Geometry

• Correlation between CT numbers and tissue parameters

• Tissue inhomogenities

• Scatter corrections, selective radiation absorption

The HG-02 IASA GRID Cluster

IASA Grid Operational Center #1

Partner of the GRNET

64 HP servers with dual Intel Xeon (3.4 GHz)

The HG-02-IASA Storage Array

Concluding Remarks

High Performance Computing environment plays an important role for Medical Image Applications:

Tomographic Image Reconstruction

• Parallelization of Filtered Back Projection Algorithms
• Acceleration of Iterative Processes
• ANN Applications

Monte Carlo Simulation

• Emission Tomography (SPECT, PET)
• Optical Transport Processes
• Radiotherapy Treatment

Integrative approach to high-performance biomedical problem solving environments on the Grid.